

Zero-Shot Instruction Following in RL via Structured LTL Representations

Mathias Jackermeier¹ Mattia Giuri¹ Jacques Cloete² Alessandro Abate¹

Abstract

We study instruction following in multi-task reinforcement learning, where an agent must zero-shot execute novel tasks not seen during training. In this setting, linear temporal logic (LTL) has recently been adopted as a powerful framework for specifying structured, temporally extended tasks. While existing approaches successfully train generalist policies, they often struggle to effectively capture the rich logical and temporal structure inherent in LTL specifications. In this work, we address these concerns with a novel approach to learn *structured* task representations that facilitate training and generalisation. Our method conditions the policy on sequences of Boolean formulae constructed from a finite automaton of the task. We propose a hierarchical neural architecture to encode the logical structure of these formulae, and introduce an attention mechanism that enables the policy to reason about future subgoals. Experiments in a variety of complex environments demonstrate the strong generalisation capabilities and superior performance of our approach.

1. Introduction

Recent years have witnessed remarkable progress in training artificial intelligence agents to follow arbitrary instructions (Luketina et al., 2019; Liu et al., 2022; Paglieri et al., 2025; Klissarov et al., 2025). A key consideration in this line of work is the *type* of instruction to provide to the agent. While a long line of research has investigated tasks expressed in natural language (Oh et al., 2017; Goyal et al., 2019; Hill et al., 2020; Carta et al., 2023), there recently has been increased interest in training agents to follow instructions specified in *formal* language (Jothimurugan et al., 2021; Vaezipoor et al., 2021; Jackermeier & Abate, 2025). Compared to natural language, formal specifications offer several advantages: they facilitate the training process by

¹Department of Computer Science, University of Oxford
²Oxford Robotics Institute, University of Oxford. Correspondence to: Mathias Jackermeier <mathias.jackermeier@cs.ox.ac.uk>.

Preprint. February 17, 2026.

enabling the automatic construction of task-specific reward functions, they explicitly expose task structure via their compositional syntax, and they are grounded in well-defined semantics. This makes formal instruction languages especially appealing in safety-critical settings, in which specifying unambiguous tasks is important (León et al., 2021).

One particular formal language that has emerged as an expressive formalism for specifying tasks in reinforcement learning (RL) is *linear temporal logic* (LTL; Pnueli, 1977). LTL instructions are defined over a set of *atomic propositions*, corresponding to high-level events that can hold true or false at each state of the environment. These atomic propositions are combined using logical and temporal operators, which allow for the specification of complex, temporally extended behaviour in a compositional manner. Recent work has exploited the connection between LTL and corresponding automata structures (typically variants of Büchi automata; Büchi, 1966), which provide an automatic way to monitor task progress, to train generalist policies capable of executing arbitrary LTL instructions at test time (Qiu et al., 2023; Jackermeier & Abate, 2025; Guo et al., 2025).

In this paper, we develop a novel approach to train generalist LTL-conditioned policies. Our method is designed to explicitly model the rich logical and temporal structure of LTL specifications, in order to yield *structured* task representations that accelerate learning and enable improved generalisation. We obtain these representations by translating transitions in the automaton into equivalent Boolean formulae, which provide succinct, compositional descriptions of the logical conditions required to make progress towards a given task. We propose a hierarchical neural architecture to encode these formulae, and introduce an attention mechanism that allows the policy to reason about future subgoals, enabling more effective planning. Our main contributions are as follows:

- we propose representing LTL instructions as sequences of Boolean formulae constructed from transitions in the corresponding Büchi automaton;
- we develop a structured representation learning approach to embed these sequences of formulae, based on a hierarchical neural architecture coupled with a temporal attention mechanism;

- we introduce a novel environment with complex logical structure, which allows us to systematically study the effectiveness of our approach across challenging LTL specifications;
- lastly, we conduct an extensive empirical evaluation demonstrating that our method achieves state-of-the-art results and significantly outperforms existing approaches across a wide range of tasks.

2. Related Work

Significant research effort has explored LTL as a task specification language for RL agents. Many works focus on training agents to satisfy a *single* specification that is fixed throughout training and evaluation (Sadigh et al., 2014; Hasanbeig et al., 2018; Camacho et al., 2019; Hahn et al., 2019; Bozkurt et al., 2020; Cai et al., 2021; Shao & Kwiatkowska, 2023; Voloshin et al., 2023; Le et al., 2024; Shah et al., 2025). In contrast, we aim to learn a general multi-task policy that can zero-shot execute arbitrary LTL instructions at test time.

This more challenging problem has received considerable interest in recent years. An early method was proposed by Kuo et al. (2020), who compose recurrent neural networks (RNNs) mirroring the LTL formula structure to produce a task representation. However, this approach requires learning a non-stationary policy (i.e. with memory), which is generally challenging (Vaezipoor et al., 2021). Another line of research instead decomposes LTL specifications into subtasks, which are then completed sequentially by a goal-conditioned policy (Araki et al., 2021; León et al., 2021; 2022; Qiu et al., 2023; Liu et al., 2024; Guo et al., 2025). While this simplifies the learning process, such methods can exhibit *myopic* behaviour: since the policy only considers a single subgoal at a time, it may not be able to produce a globally optimal solution. In contrast, our method conditions the policy on the entire sequence of Boolean formulae that need to be satisfied in order to complete the task.

Vaezipoor et al. (2021) introduce LTL2Action, which directly encodes the LTL formula’s syntax tree using a graph neural network (GNN) and employs LTL progression (Bacchus & Kabanza, 2000) to continuously update the task representation. While this allows for generalisation to some extent, the primary drawback of this method is that it requires the policy to *learn* the semantics of temporal operators. Instead, we construct Büchi automata to explicitly capture the temporal structure of tasks. Reasoning over Büchi automata furthermore allows us to naturally handle infinite-horizon tasks, which LTL2Action does not support.

Automata have previously been explored for training generalist LTL-conditioned policies. However, our work differs in how the task is represented and processed. Instead of

learning a policy conditioned myopically on single atomic propositions (Qiu et al., 2023), or on sequences of unstructured sets of assignments (Jackermeier & Abate, 2025), we propose to construct semantically meaningful Boolean formulae from the transitions in the automaton, and learn a policy conditioned on sequences thereof. This provides a more explicit and structured representation of the task transition dynamics. Additionally, we incorporate information about future subgoals via a novel attention mechanism. Guo et al. (2025) recently proposed a safe RL formulation coupled with a specialised observation reduction technique. However, their approach is myopic and furthermore limited to environments in which such a manually designed observation reduction is applicable. In contrast, our method does not require such assumptions. Concurrent work (Cloete et al., 2026) explores scaling LTL-conditioned RL to domains with possibly infinite numbers of propositions by treating them as parameterised predicates. This is a fundamentally different problem, and only applies to domains that naturally admit parameterised predicates, whereas we focus on improved structured task representations for arbitrary environments.

3. Background

Reinforcement Learning. We formally model reinforcement learning (RL) environments as Markov decision processes (MDPs). An MDP is defined as a tuple $\mathcal{M} = (\mathcal{S}, \mathcal{A}, p, r, \gamma, \rho_0)$, where \mathcal{S} is the state space, \mathcal{A} is the action space, $p : \mathcal{S} \times \mathcal{A} \times \mathcal{S} \rightarrow [0, 1]$ is the transition probability function, $r : \mathcal{S} \times \mathcal{A} \times \mathcal{S} \rightarrow \mathbb{R}$ is the reward function, $\gamma \in [0, 1]$ is the discount factor, and ρ_0 is the initial state distribution. A (memoryless) policy $\pi : \mathcal{S} \rightarrow \Delta(\mathcal{A})$ maps states to probability distributions over actions. The goal of RL is to find a policy π that maximises the expected discounted return $J(\pi) = \mathbb{E}_{\tau \sim \pi} [\sum_{t=0}^{\infty} \gamma^t r_t]$, where $\tau = (s_0, a_0, r_0, s_1, \dots)$ is a trajectory generated by following π starting from $s_0 \sim \rho_0$, that is, $a_t \sim \pi(\cdot | s_t)$, $s_{t+1} \sim p(\cdot | s_t, a_t)$, and $r_t = r(s_t, a_t, s_{t+1})$. The value function of π is defined as $V^\pi(s) = \mathbb{E}_{\tau \sim \pi} [\sum_{t=0}^{\infty} \gamma^t r_t | s_0 = s]$, i.e. the expected discounted return of π starting from state s .

Linear Temporal Logic. We use linear temporal logic (LTL; Pnueli, 1977) to specify tasks for RL agents. LTL formulae are defined over a set of atomic propositions (AP), which represent basic properties of the environment such as “object A is at location X ” or “the agent is in the green region”. LTL formulae are defined recursively as

$$\varphi ::= \top \mid p \mid \neg \varphi \mid \varphi \wedge \psi \mid X \varphi \mid \varphi \cup \psi$$

where \top denotes true, $p \in AP$ is an atomic proposition, φ and ψ are themselves LTL formulae, \neg (negation) and \wedge (conjunction) are standard Boolean connectives (from which others like \vee , \rightarrow , \leftrightarrow can be derived), and X (next) and \cup

(until) are temporal operators. From these, the common temporal operators $F\varphi \equiv \top \cup \varphi$ (eventually or finally) and $G\varphi \equiv \neg F \neg \varphi$ (always or globally) can be derived. Intuitively, $\varphi \cup \psi$ is true if ψ becomes satisfied at some time step t and φ is true at all previous time steps. Accordingly, $F\varphi$ simply states that φ has to be true *eventually*, whereas $G\varphi$ requires φ to be true at every time step.

Formally, LTL semantics are defined over infinite traces of *truth assignments* $\sigma = \sigma_0 \sigma_1 \sigma_2 \dots$, where $\sigma_t \subseteq AP$ is the set of atomic propositions true at time t . We assume a (known) labelling function $L : \mathcal{S} \rightarrow 2^{AP}$, which maps MDP environment states $s \in \mathcal{S}$ to corresponding sets of true atomic propositions. A trajectory $\tau = (s_0, a_0, s_1, \dots)$ satisfies an LTL formula φ , denoted $\tau \models \varphi$, if its trace $L(s_0)L(s_1)\dots$ satisfies φ according to LTL semantics (see Appendix A). For example, the formula $\neg a \cup b$ is satisfied by exactly the trajectories where eventually b is true at some time step t (i.e. $b \in L(s_t)$), and a is false at all time steps before. LTL provides a formal and structured way to define complex tasks to RL agents, such as “eventually reach region A, and if you pick up an object on the way, you must also visit region B while avoiding region C”. The problem of training a generalist LTL-guided policy can be formalised by defining a distribution \mathcal{D} over LTL tasks. We then aim to compute the optimal task-conditioned policy

$$\pi^*(\cdot | \varphi) = \arg \max_{\pi} \mathbb{E}_{\substack{\varphi \sim \mathcal{D}, \\ \tau \sim \pi | \varphi}} [\mathbb{1}[\tau \models \varphi]]. \quad (1)$$

Büchi Automata. The semantics of LTL can equivalently be captured by Büchi automata (Büchi, 1966), which provide a more explicit way to reason about tasks. We here focus on *limit-deterministic* Büchi automata (LDAs; Sickert et al., 2016), which are defined as tuples $\mathcal{B} = (\mathcal{Q}, q_0, \Sigma, \delta, \mathcal{E}, \mathcal{F})$. $\mathcal{Q} = \mathcal{Q}_I \uplus \mathcal{Q}_A$ is a finite set of states partitioned into two subsets, $q_0 \in \mathcal{Q}$ is the initial state, $\Sigma = 2^{AP}$ is a finite alphabet, $\delta : \mathcal{Q} \times (\Sigma \cup \mathcal{E}) \rightarrow \mathcal{Q}$ is the transition function, and \mathcal{F} is the set of accepting states. We require that $\mathcal{F} \subseteq \mathcal{Q}_A$ and $\delta(q, \cdot) \in \mathcal{Q}_A$ for all $q \in \mathcal{Q}_A$. The only way to transition from \mathcal{Q}_I to \mathcal{Q}_A is by taking an ε -transition $\varepsilon \in \mathcal{E}$ (a.k.a. *jump* transition), which does not consume any input. Given an input trace σ , a *run* of \mathcal{B} is an infinite sequence of states in \mathcal{Q} starting in q_0 and respecting the transition function δ . A trace is *accepted* by \mathcal{B} if there exists a run that infinitely often visits accepting states. There exist standard algorithms, e.g. (Sickert et al., 2016), to construct an LDA \mathcal{B}_φ from an LTL formula φ such that \mathcal{B}_φ accepts exactly the traces satisfying φ .

Example 3.1. Figure 1 shows an LDA for the formula $F \text{red} \vee (F G \text{green})$. In q_0 , the agent can either choose ε_1 to transition to q_1 , from which it reaches the accepting state q_2 upon visiting an MDP state s with $\text{red} \in L(s)$. By following ε_2 , it instead has to stay in a green state forever. Note that we assume here that red and green cannot be true together.

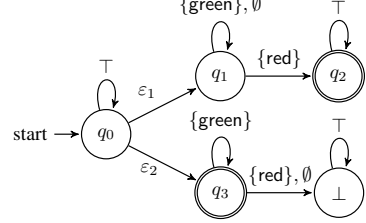


Figure 1. LDA for the LTL formula $F \text{red} \vee (F G \text{green})$.

Büchi automata are well-suited to represent LTL instructions, since they explicitly capture the memory required to execute a given task via their states. It is hence common to consider policies $\pi : \mathcal{S} \times \mathcal{Q} \rightarrow \Delta(\mathcal{A})$ conditioned not only on the current MDP state s , but also on the current LDA state q (Hasanbeig et al., 2018; Hahn et al., 2019). After each environment interaction, the automaton state is updated according to the transition function δ and the currently true propositions $L(s)$. Over the course of a trajectory, the policy can adjust its behaviour as the LDA state changes. For example, in Figure 1 the policy would aim to make red true in q_1 , but in q_3 instead try to stay in a green state.

4. Structured LTL Representations

In single-task RL, it is straightforward to condition the policy on LDA states. Since the automaton remains fixed throughout training and evaluation, one can simply train separate state-specific sub-policies, and choose the appropriate one at test time (e.g. Jothimurugan et al., 2021). However, this approach is unfeasible in multi-task RL, since the policy must generalise to novel tasks (and therefore automata states) that it has never encountered during training. The key challenge is thus to find a suitable representation of LDA states that (i) enables such generalisation, and (ii) is amenable to policy learning.

Recent work has explored various representations, such as conditioning on single atomic propositions (Qiu et al., 2023), sequences of unstructured sets of assignments (Jackermeier & Abate, 2025), or directly encoding the LTL formula syntax tree (Vaezipoor et al., 2021). However, these approaches struggle to effectively capture the rich logical and temporal structure of tasks, particularly in environments where many propositions can hold simultaneously.

As illustrated in Figure 2, we instead propose representing LDA states as *sequences of Boolean formulae*. This representation explicitly exposes the logical structure of tasks, enabling the policy to generalise compositionally. For example, it can leverage knowledge about achieving propositions a and b individually to also achieve $a \wedge b$. Furthermore, since the policy is conditioned on a *sequence* of such formulae, it can non-myopically reason about future subgoals, which may affect how it approaches the current step.

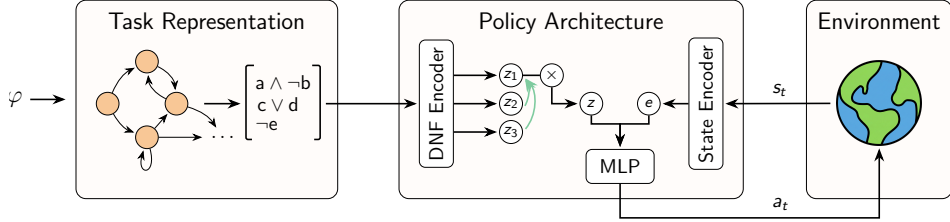


Figure 2. Overview of our method. (Left) Given an LTL instruction φ , we construct an LDBA and extract sequences of Boolean formulae representing the current automaton state. (Right) The policy is conditioned on a single formula sequence. It processes formulae with a hierarchical DNF encoder and a temporal attention mechanism to reason about future subgoals. The latent task representation z is concatenated with the encoded MDP state s_t and mapped to an action a_t via an actor MLP.

Intuitively, these sequences of Boolean formulae align with *accepting runs* in the LDBA, informing the policy of the high-level steps required to complete the task. We design a procedure to automatically construct such sequences from the LDBA (Section 4.1), and propose a specialised neural network architecture that leverages the rich information in these sequences to yield *structured* learned task representations (Section 4.2). Further details on the training procedure are given in Section 4.3. Finally, Section 4.4 describes the test-time execution, where the policy is conditioned on sequences extracted from the current task’s LDBA and updates dynamically as the automaton state evolves.

4.1. Representing LDBA States with Boolean Formulae

Given an LDBA \mathcal{B}_φ and state q , we aim to identify behaviour that will lead to satisfying the LTL instruction. Since φ is satisfied exactly when the agent visits accepting states infinitely often, we first enumerate possible ways to reach an *accepting cycle* in \mathcal{B}_φ , i.e. a cycle with at least one accepting state. This can be achieved with a simple depth-first search (DFS) starting from q (Algorithm 1 of Jackermeier & Abate (2025); see Appendix B for details).

The DFS yields a set of accepting runs $\rho_i = (q, q_1, \dots)$ that correspond to different ways of achieving φ . For each run ρ_i , we construct a sequence of Boolean formulae that captures the high-level goals the agent must complete in order to follow the run, and hence satisfy the LTL task. Specifically, in order to transition from q_i to q_{i+1} , the agent must achieve an assignment $\alpha_i \subseteq AP$ of atomic propositions that satisfies the transition condition $\delta(q_i, \alpha_i) = q_{i+1}$, while avoiding transitions to other states (excluding self-loops). We represent this with two Boolean formulae β_i^+ and β_i^- that satisfy

$$\begin{aligned} \forall \alpha \in \mathbb{A}. \alpha \models \beta_i^+ &\iff \delta(q_i, \alpha) = q_{i+1}, \\ \forall \alpha \in \mathbb{A}. \alpha \models \beta_i^- &\iff \delta(q_i, \alpha) \notin \{q_i, q_{i+1}\}, \end{aligned}$$

where $\mathbb{A} = \{L(s) : s \in \mathcal{S}\} \subseteq 2^{AP}$ is the set of possible assignments in the MDP. Intuitively, β_i^+ is only true for the assignments that transition from q_i to q_{i+1} , whereas β_i^- captures the assignments that must be avoided in order to

avoid transitioning to other states. Boolean formulae can be much more succinct than explicitly enumerating sets of assignments, as we demonstrate with the following example.

Example 4.1. Consider an MDP with propositions $AP = \{a, b, c, d\}$ in which all combinations of propositions can hold true at the same time (i.e. $\mathbb{A} = 2^{AP}$). Assume we have an LDBA in which we can transition from state q_0 to q_1 via any of the assignments in the set

$$A = \{\{a\}, \{a, b\}, \{a, d\}, \{a, b, d\}\}.$$

The formula $\beta_0^+ \equiv a \wedge \neg c$ succinctly represents exactly this set of assignments.

Constructing Boolean formulae. We construct formulae β_i^+ and β_i^- for each step i in a run as follows: we first identify the relevant sets of assignments A_i^+ and A_i^- from the transition function δ , that is, $A_i^+ = \{\alpha \in \mathbb{A} : \delta(q_i, \alpha) = q_{i+1}\}$ and $A_i^- = \{\alpha \in \mathbb{A} : \delta(q_i, \alpha) \notin \{q_i, q_{i+1}\}\}$. We could then trivially construct formulae in *disjunctive normal form* (DNF) by exhaustively building a formula for each assignment. However, this representation is as verbose as simply listing the assignments themselves; instead, we aim to find small, semantically meaningful formulae that capture the assignments while enabling generalisation at test time.

Constructing minimal Boolean formulae is a well-studied problem in formal logic and the minimisation of digital circuits. We employ the widely used Quine-McCluskey algorithm (Quine, 1952; McCluskey, 1956) to compute minimal DNF representations of β_i^+ and β_i^- . This algorithm takes as input a set of satisfying assignments S and a set of non-satisfying assignments N to produce a minimal (in terms of number of disjunctions and conjunctions) DNF formula that evaluates to true for assignments in S and to false for assignments in N . We set $S = A_i^+$ (or A_i^-) and $N = \mathbb{A} \setminus S$ to yield the formulae β_i^+ and β_i^- , respectively.

Note that an accepting run may contain an ε -transition representing a non-deterministic choice. These transitions do not consume input and hence require no Boolean formula; we instead represent them with a special token β_ε that we handle separately in our policy architecture (see Section 4.2).

4.2. Structured Representation Learning

Effectively conditioning a policy on the sequences derived in Section 4.1 presents two challenges: (i) the Boolean formulae possess hierarchical logical structure that unstructured embeddings may fail to capture, and (ii) the sequences vary in length depending on the task’s complexity. To address these challenges, we propose a hierarchical architecture to encode the structure of individual formulae and a temporal attention mechanism to process the sequence of subgoals. This is illustrated in Figure 2 (right).

Formally, we denote by $\zeta = ((\beta_1^+, \beta_1^-), (\beta_2^+, \beta_2^-), \dots)$ a sequence of Boolean formula pairs extracted from an accepting run. Our policy $\pi(a | s, \zeta)$ takes as input the current MDP state s and such a target sequence ζ . Note that while there may be multiple accepting runs for a given LDBA state, the policy is conditioned on a *single* formula sequence at any given time; we detail the run selection procedure in Section 4.4.

Embedding Boolean formulae. There are a number of straightforward choices to embed Boolean formulae, such as token-level sequence encoders (e.g. LSTMs or GRUs) or structure-aware encoders, e.g. applying a GNN to a syntax tree representation of the formula (Evans et al., 2018; Crouse et al., 2020). Rather than using such general methods, we exploit two key features of the formulae encountered by our policy: (i) they only contain propositions from AP , and (ii) they are guaranteed to be in DNF by construction.

Specifically, a formula in DNF consists of a *disjunction* of one or more *clauses*, i.e. has the form $\bigvee_{i=1}^n \bigwedge_{j=1}^{m_i} l_{ij}$, where l_{ij} is a possibly negated atomic proposition. We process DNF formulae in a hierarchical fashion as follows. Our policy associates a trainable embedding $e_a \in \mathbb{R}^d$ with each proposition $a \in AP$. Negated propositions are first processed with a learned linear projection layer, and literals in a clause are then aggregated into a single representation via a permutation-invariant set encoder (since the order of literals does not affect the semantics). In particular, we use a simple DeepSets encoder (Zaheer et al., 2017) consisting of a sum followed by a learned non-linear transformation. The resulting clause embeddings are aggregated again on the disjunction level by another DeepSets encoder, yielding the overall formula representation z . Formally, we have

$$z = f_{\vee} \left(\sum_{i=1}^n f_{\wedge} \left(\sum_{j=1}^{m_i} \Pi(e_{a_{ij}}) \right) \right),$$

where f_{\vee} and f_{\wedge} are the non-linear transformations, and Π denotes the projection layer if l_{ij} is negated, and the identity function otherwise. Finally, this does not apply to the special β_{ε} token, for which we instead learn a separate embedding. We give more details on how we handle ε -transitions below.

Attending to future subgoals. In order to produce optimal behaviour, the policy may need to consider future subgoals rather than myopically focusing only on the first step of the sequence ζ . To illustrate, consider a simple sequential task where the agent needs to achieve a and then b . Depending on the underlying MDP, there may be different ways of making a true, some of which might render b infeasible (e.g. if the agent enters a room in order to achieve a that locks upon entry). At the same time, the first step of the sequence generally contains the most important information, since this is the goal the agent is currently trying to achieve. We model this intuition with a temporal attention mechanism that allows the policy to contextualise the representation of the current step by attending to future subgoals.

In particular, let z_i^+ and z_i^- denote the embedding of β_i^+ and β_i^- , respectively. We first concatenate these embeddings to obtain the overall encoding of step i as $z_i = [z_i^+; z_i^-]$. We use the first step z_1 as the query to attend to the entire sequence using single-head scaled dot-product attention (Vaswani et al., 2017), which computes the output

$$h = \left[\text{softmax} \left(\frac{qK^{\top}}{\sqrt{d_k}} \right) V \right] W^O,$$

where $q = z_1 W^Q$ is the query vector, and $K, V \in \mathbb{R}^{T \times d_k}$ are the key and value matrices obtained by projecting the sequence embeddings $z_{1:T}$ using W^K and W^V , respectively. W^O is the output projection matrix. Intuitively, h captures how future formulae in the sequence modulate the current goal z_1 . We obtain the final contextualised goal representation as $\tilde{z}_1 = \text{LayerNorm}(z_1 + h)$ (Ba et al., 2016). Since pure attention does not preserve sequential information, we employ ALiBi (Press et al., 2021) to bias the attention towards nearby steps. Specifically, before applying the softmax, we subtract a linear penalty $m \cdot (i-1)$ from the unnormalised attention score for step i (where $i \geq 2$), with $m > 0$ being a fixed hyperparameter. This intuitively captures that steps further in the future tend to have less influence on the immediate subgoal.

Finally, note that formula sequences constructed from accepting runs are technically infinite, since they describe accepting cycles in the automaton. Similar to previous work (Jackermeier & Abate, 2025), we truncate sequences after repeating the looping subsequence (corresponding to the accepting cycle) k times, where $k \in \mathbb{N}$ is a hyperparameter.

Full policy architecture. As depicted in Figure 2 (right), our policy not only processes the formula sequence, but also encodes the current MDP state via a *state encoder*. This is either a multilayer perceptron (MLP) or convolutional neural network (CNN), depending on the environment. The contextualised formula sequence embedding \tilde{z}_1 is concatenated with the encoded MDP state and fed into a final *actor* MLP, which produces a distribution over actions.

We handle ε -transitions in the LDBA by augmenting the action space of the policy with designated ε -actions, as is commonly done (Hasanbeig et al., 2018; Voloshin et al., 2023). These do not perform an action in the MDP, but instead simply update the current LDBA state to the target of the corresponding ε -transition. Our policy hence produces a mixture distribution, where it takes an ε -action with parameter p and otherwise samples from its distribution over MDP actions. Note that ε -actions are naturally only enabled if the current step of the sequence ζ is an ε -transition.

4.3. Training Procedure

We optimize the parameters of our model end-to-end via goal-conditioned RL (Liu et al., 2022). That is, we sample a random Boolean formula sequence ζ at the beginning of each training episode. We then execute a rollout with the policy conditioned on ζ , assigning a positive reward of $+1$ to an episode if the agent successfully sequentially satisfies all formulae β_i^+ . If the agent at any step i instead satisfies the currently active β_i^- , we assign a negative reward of -1 . This reward structure encourages the policy to satisfy formula sequences that lead to accepting cycles, and hence approximates Equation (1). We use *proximal policy optimization* (PPO; Schulman et al., 2017) to jointly optimise the policy and learn a value function V^π .

Since the agent is unlikely to be able to successfully complete complex sequences of formulae in the beginning of training, we employ *curriculum learning* to improve training convergence. We design a generic training curriculum consisting of increasingly challenging sequences of Boolean formulae. For example, we start the training process with simple single-step sequences requiring the agent to make a single proposition true. Once the policy is successful on these tasks, we move on to more complicated formula sequences. Further details on curriculum learning are given in Appendix C.2. We note that Jackermeier & Abate (2025) previously demonstrated the effectiveness of curriculum learning for training generalist LTL-conditioned policies.

4.4. Test-time Policy Execution

At test time, we are given a new LTL instruction φ and build a corresponding LDBA \mathcal{B}_φ . We then perform the DFS described in Section 4.1 to extract a set of Boolean formula sequences $\{\zeta_1, \dots, \zeta_n\}$ from the initial state q_0 . We use the trained *value function* V^π to select the formula sequence that the policy is approximately most likely able to achieve from the current MDP state s , i.e. we compute

$$\zeta^* = \arg \max_{\zeta_i} V^\pi(s, \zeta).$$

Intuitively, ζ^* corresponds to the path through the automaton with the highest likelihood of success. The value function, which is a by-product of the training algorithm, natu-

rally estimates (a lower bound of) this likelihood and is hence an appropriate choice for selecting a formula sequence. We then execute the trained policy π conditioned on ζ^* , i.e. continuously sample actions $a_t \sim \pi(\cdot | s_t, \zeta^*)$, until the LDBA state changes, upon which we recompute and update the formula sequence used to condition the policy.

5. Experiments

We evaluate our method across diverse environments, including high-dimensional domains with continuous action spaces. We aim to answer the following research questions:¹

(Q1) Can our approach effectively zero-shot generalise to unseen LTL instructions, particularly those requiring compositional reasoning? **(Q2)** How does our method compare to state-of-the-art baselines in terms of sample efficiency and asymptotic performance? **(Q3)** What is the individual impact of the proposed hierarchical DNF encoder and temporal attention mechanism?

5.1. Experimental Setup

Environments. We conduct experiments in *ZoneEnv* (Vaeziropoor et al., 2021), a well-established high-dimensional robotic navigation environment, in which the agent observes differently coloured zones via a lidar sensor. The colours correspond to the atomic propositions, which hold true if the agent is in a zone of the corresponding colour. The zones are positioned randomly at the beginning of each episode, and the agent must navigate between them using continuous actions. We furthermore introduce the *Warehouse* environment, which admits complex logical specifications and thus allows us to systematically evaluate the compositional reasoning abilities of our method. It consists of an agent navigating three fixed regions while interacting with two types of objects: *crates* and *vases*. The positions of these objects are randomly sampled, and the agent observes their location relative to itself via a lidar sensor (similar to *ZoneEnv*). The environment features a hybrid action space: the agent can both apply a continuous movement action and choose from a set of discrete actions to pick up and drop objects. Atomic propositions capture if the agent is currently located within one of the designated regions, and which objects it is carrying.

Notably, the warehouse environment supports complex combinations of atomic propositions holding true at the same time. For example, if the agent is in region A while carrying both a vase and crate, all three of these propositions hold true. Completing tasks in the warehouse environment thus requires the agent to reason compositionally about interactions between propositions. See Appendix C.1 for further details on the environments, including visualisations.

¹Code will be released upon publication.

Baselines. We compare our approach, named StructLTL, to state-of-the-art approaches for learning generalist LTL-conditioned policies. LTL2Action (Vaezipoor et al., 2021) directly encodes the syntax tree of a given specification using a GNN. While this theoretically allows LTL2Action to exploit logical structure similarly to our method, it needs to learn policy behaviour from the syntax of specifications alone, which is challenging. We furthermore compare to DeepLTL (Jackermeier & Abate, 2025), the state-of-the-art non-myopic approach based on Büchi automata. DeepLTL represents tasks as *reach-avoid* sequences of unstructured assignments, which are embedded with an RNN. We do not compare to the myopic method GCRL-LTL (Qiu et al., 2023), which has been shown to be significantly outperformed by DeepLTL, nor do we consider the recent method GenZ-LTL (Guo et al., 2025), since this relies on the limiting assumption that the observation space can be partitioned into homogeneous proposition-specific observations. Our method does not require such an assumption, which in particular does not hold in the complex Warehouse environment.

Tasks. We consider diverse tasks of varying complexity to evaluate the trained policies. We differentiate between *finite-horizon* (i.e. co-safety) tasks, which can be completed in a finite number of steps, and *infinite-horizon* tasks, which specify recurrent behavior that the agent must execute indefinitely. Our tasks span a wide range of environment-specific behaviour, such as reaching and avoiding different zones in ZoneEnv, or transporting objects between regions in the Warehouse environment. They furthermore make use of complex LTL constructs, such as implications to specify *response* tasks and nested temporal operators. As an example, task φ_{13} of our evaluation is given by

$$\begin{aligned} & (\text{crate} \rightarrow (\text{crate} \cup \text{region_b})) \\ & \text{U } (\text{crate} \wedge \text{region_b} \wedge (\text{region_b} \cup (\neg \text{crate} \wedge \text{region_b}))), \end{aligned}$$

which can be read as “Pick up a crate and place it in region B. After you have picked up the crate, you must not put it down again, until you have reached the region.” We provide a full list of evaluation specifications in Appendix C.4.

Evaluation protocol. DeepLTL and StructLTL are trained with the same generic training curriculum (see Appendix C.2 for further details). LTL2Action originally does not employ curriculum training, but we found this to be beneficial and thus use an adapted training curriculum for a fair comparison. We train for 20M environment interaction steps in ZoneEnv, and 200M steps in Warehouse. All methods that we consider are based on PPO (Schulman et al., 2017), and we provide detailed hyperparameters in Appendix C.3. We follow standard practice (Qiu et al., 2023; Jackermeier & Abate, 2025; Guo et al., 2025) and report both success rates and number of steps until successful completion for

finite-horizon tasks. For infinite-horizon tasks, we evaluate the number of visits to accepting states, i.e. how often the policy managed to complete an accepting cycle over a fixed evaluation horizon of 1000 steps. Note that LTL2Action does not support infinite-horizon tasks, and we thus omit it for these results. All our results are averaged over 10 random seeds and 512 episodes per seed, and we provide standard deviations and/or confidence intervals.

5.2. Results

Figure 3 shows evaluation curves averaged over finite-horizon tasks over training. Table 1 furthermore lists results of the trained policies on both finite- and infinite-horizon specifications, and we plot trajectories produced by StructLTL in Appendix E.

We observe that StructLTL consistently achieves high success rates in finite-horizon tasks, with more than 95% in most cases. This is true not only for the simpler specifications in ZoneEnv, but also for complex tasks requiring compositional reasoning in the Warehouse environment (Q1). In comparison to the baselines, we overall achieve significantly higher performance, particularly on the complex tasks $\varphi_{12} - \varphi_{16}$ where baseline methods struggle (Q2). These results highlight the benefits of our structured representations: whereas our approach represents complex combinations of atomic propositions via succinct Boolean formulae, DeepLTL struggles to handle the combinatorial explosion of assignments. We investigate the robustness of our approach to increasing numbers of possible assignments further in Appendix D.3. While LTL2Action does not operate on the assignment level, and is hence not susceptible to this same problem, we observe that it generally underperforms even on simpler tasks. This is likely because LTL2Action must learn the complex temporal dynamics of LTL specifications from scratch given only a syntax tree representation, whereas we and DeepLTL reason about the structure of the corresponding Büchi automaton.

Furthermore, we see that our approach is also generally more *efficient*, i.e. manages to complete tasks in fewer steps on average. This efficiency advantage is consistent with the design of our temporal attention mechanism: by attending to future subgoals, the policy can learn to avoid myopic decisions that lead to longer solution paths. The evaluation curves in Figure 3 additionally highlight the sample efficiency of our method in comparison to the baselines. The results on infinite-horizon tasks paint a similar picture: our approach consistently completes more accepting cycles in the LDBA for all but one formula, suggesting that it is both better and more efficient at achieving challenging infinite-horizon specifications.

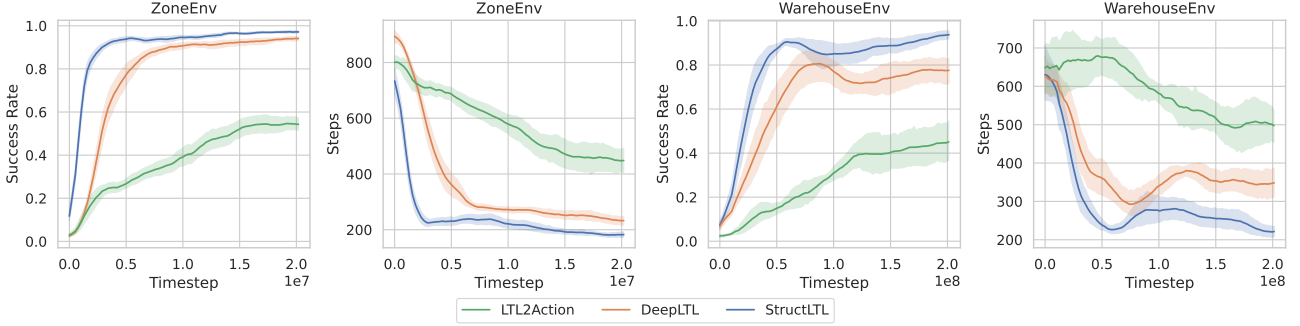


Figure 3. Evaluation curves on finite-horizon tasks over training. We report averages over the entire set of finite-horizon evaluation tasks, computed over 50 episodes per task. Shaded areas indicate 90% confidence intervals over 10 random seeds.

Table 1. Evaluation results of trained policies on finite- and infinite-horizon tasks. We report both success rates and average number of steps until successful completion for finite-horizon tasks. For infinite-horizon tasks, we report the average number of visits to accepting states over 1000 timesteps. Results are averaged over 10 seeds and 512 episodes per seed, with \pm indicating standard deviation over seeds.

Finite Horizon												Infinite Horizon			
												Average Visits (\uparrow)			
		Success Rate (\uparrow)			Average Steps (\downarrow)										
φ	LTL2Action	DeepLTL	StructLTL	LTL2Action	DeepLTL	StructLTL	ψ	DeepLTL	StructLTL	ψ_1	ψ_2	ψ_3	ψ_4	ψ_5	ψ_6
ZoneEnv	φ_1	0.49 \pm 0.18	0.96 \pm 0.03	0.98 \pm 0.01	469.75 \pm 044.81	288.28 \pm 49.65	224.08 \pm 21.88	ψ_1	4.77 \pm 1.41	6.72 \pm 0.88					
	φ_2	0.17 \pm 0.11	0.92 \pm 0.05	0.97 \pm 0.01	386.17 \pm 111.31	276.03 \pm 40.25	217.28 \pm 14.07	ψ_2	1.50 \pm 0.54	2.83 \pm 0.34					
	φ_3	0.62 \pm 0.24	0.98 \pm 0.01	0.99 \pm 0.00	406.99 \pm 060.10	237.71 \pm 34.70	183.76 \pm 15.08	ψ_3	560.58 \pm 194.99	633.33 \pm 122.02					
	φ_4	0.52 \pm 0.22	0.91 \pm 0.02	0.96 \pm 0.02	338.67 \pm 095.52	179.49 \pm 20.48	148.41 \pm 10.80	ψ_4	404.11 \pm 150.88	511.48 \pm 070.50					
	φ_5	0.63 \pm 0.24	0.93 \pm 0.04	0.97 \pm 0.01	367.88 \pm 100.70	209.14 \pm 37.51	152.67 \pm 18.86	ψ_5	467.83 \pm 123.41	606.67 \pm 082.93					
	φ_6	0.84 \pm 0.20	0.97 \pm 0.02	0.99 \pm 0.01	155.33 \pm 036.08	130.78 \pm 19.34	105.50 \pm 07.35	ψ_6	475.01 \pm 135.77	624.44 \pm 093.83					
Warehouse	φ_7	0.98 \pm 0.02	0.98 \pm 0.01	0.99 \pm 0.01	226.31 \pm 018.68	196.46 \pm 007.90	202.05 \pm 12.89	ψ_7	2.52 \pm 0.33	2.78 \pm 00.12					
	φ_8	0.56 \pm 0.41	0.95 \pm 0.02	0.95 \pm 0.02	346.16 \pm 135.52	160.20 \pm 019.88	173.22 \pm 38.42	ψ_8	13.84 \pm 5.11	15.92 \pm 12.01					
	φ_9	0.46 \pm 0.38	0.99 \pm 0.03	0.99 \pm 0.01	390.74 \pm 129.51	225.65 \pm 007.59	252.65 \pm 25.03	ψ_9	2.32 \pm 0.60	3.19 \pm 00.29					
	φ_{10}	0.36 \pm 0.34	0.88 \pm 0.07	0.80 \pm 0.15	387.15 \pm 062.66	353.14 \pm 053.83	371.19 \pm 33.75	ψ_{10}	2.07 \pm 1.18	3.93 \pm 00.64					
	φ_{11}	0.42 \pm 0.46	0.91 \pm 0.10	0.99 \pm 0.00	331.33 \pm 197.05	185.35 \pm 049.94	126.82 \pm 05.73	ψ_{11}	823.49 \pm 197.13	880.60 \pm 055.70					
	φ_{12}	0.63 \pm 0.45	0.58 \pm 0.40	0.97 \pm 0.04	304.32 \pm 135.13	305.16 \pm 129.82	193.26 \pm 22.89	ψ_{12}	433.90 \pm 257.90	656.79 \pm 249.07					
	φ_{13}	0.41 \pm 0.42	0.67 \pm 0.31	0.95 \pm 0.08	220.78 \pm 076.43	150.12 \pm 032.54	139.54 \pm 10.08	ψ_{13}	650.87 \pm 320.31	682.62 \pm 215.48					
	φ_{14}	0.12 \pm 0.32	0.57 \pm 0.26	0.84 \pm 0.19	573.21 \pm 101.04	430.54 \pm 092.54	329.32 \pm 56.80	ψ_{14}	219.22 \pm 299.84	351.43 \pm 207.41					
	φ_{15}	0.15 \pm 0.29	0.66 \pm 0.34	0.96 \pm 0.04	378.20 \pm 078.95	210.27 \pm 080.66	151.14 \pm 07.93	ψ_{15}	783.72 \pm 194.56	577.07 \pm 294.88					
	φ_{16}	0.06 \pm 0.11	0.52 \pm 0.33	0.88 \pm 0.27	613.39 \pm 113.26	445.41 \pm 086.08	300.02 \pm 35.27	ψ_{16}	575.43 \pm 300.78	857.86 \pm 048.45					

Ablation studies. To better understand the source of our method’s performance, we conduct ablation studies analysing the impact of the hierarchical DNF encoder and the temporal attention mechanism in Appendix D (Q3). We find that both components have a significant impact on performance and perform better than simpler baselines.

6. Conclusion and Future Work

We presented StructLTL, a novel approach for learning generalist policies to follow LTL instructions based on structured task representations. Our method exploits the structure of Büchi automata constructed from a given specification, extracting sequences of Boolean formulae that succinctly represent different ways of achieving the task. These formulae are encoded with a specialised hierarchical neural network architecture, and we furthermore introduce a temporal attention mechanism to enable non-myopic reasoning about future subgoals. In contrast to previous methods, our structured representations effectively capture interactions be-

tween atomic propositions, thereby enabling compositional generalisation. We demonstrated that our approach can effectively zero-shot generalise to unseen LTL instructions and outperforms state-of-the-art methods across complex environments and specifications.

There are several promising directions for future work. First, it would be valuable to investigate techniques such as hindsight experience replay (Andrychowicz et al., 2017; Voloshin et al., 2023) to improve the sample efficiency and performance of our method. Furthermore, future work could apply our approach to real-world robotic domains, where the labelling function L (which maps from observations to atomic propositions) may be unknown. Promising ideas in this direction include jointly learning the labelling function from visual or sensory input, or leveraging pre-trained foundation models as high-level event detectors. More broadly, we expect formal specification languages to become increasingly relevant as AI systems are deployed in safety-critical domains where unambiguous task specification is essential.

Impact Statement

This paper presents work whose goal is to advance the field of Machine Learning. There are many potential societal consequences of our work, none which we feel must be specifically highlighted here.

Acknowledgements

This work was supported by the UKRI Erlangen AI Hub on Mathematical and Computational Foundations of AI (No. EP/Y028872/1). MJ and JC are funded by the EPSRC Centre for Doctoral Training in Autonomous Intelligent Machines and Systems (EP/S024050/1).

References

Andrychowicz, M., Wolski, F., Ray, A., Schneider, J., Fong, R., Welinder, P., McGrew, B., Tobin, J., Pieter Abbeel, O., and Zaremba, W. Hindsight Experience Replay. In *Advances in Neural Information Processing Systems*, volume 30, 2017.

Araki, B., Li, X., Vodrahalli, K., Decastro, J., Fry, M., and Rus, D. The Logical Options Framework. In *Proceedings of the 38th International Conference on Machine Learning*, pp. 307–317, 2021.

Ba, J. L., Kiros, J. R., and Hinton, G. E. Layer Normalization. *arXiv*, 2016.

Bacchus, F. and Kabanza, F. Using temporal logics to express search control knowledge for planning. *Artificial Intelligence*, 116(1):123–191, 2000. ISSN 0004-3702. doi: 10.1016/S0004-3702(99)00071-5.

Bozkurt, A. K., Wang, Y., Zavlanos, M. M., and Pajic, M. Control Synthesis from Linear Temporal Logic Specifications using Model-Free Reinforcement Learning. In *2020 IEEE International Conference on Robotics and Automation (ICRA)*, pp. 10349–10355, 2020. doi: 10.1109/ICRA40945.2020.9196796.

Büchi, J. R. Symposium on Decision Problems: On a Decision Method in Restricted Second Order Arithmetic. In *Studies in Logic and the Foundations of Mathematics*, volume 44 of *Logic, Methodology and Philosophy of Science*, pp. 1–11. Elsevier, January 1966. doi: 10.1016/S0049-237X(09)70564-6.

Cai, M., Xiao, S., Li, B., Li, Z., and Kan, Z. Reinforcement Learning Based Temporal Logic Control with Maximum Probabilistic Satisfaction. In *2021 IEEE International Conference on Robotics and Automation (ICRA)*, pp. 806–812, 2021. doi: 10.1109/ICRA48506.2021.9561903.

Camacho, A., Icarte, R. T., Klassen, T. Q., Valenzano, R. A., and McIlraith, S. A. LTL and beyond: Formal languages for reward function specification in reinforcement learning. In *Proceedings of the Twenty-Eighth International Joint Conference on Artificial Intelligence, IJCAI 2019*, pp. 6065–6073, 2019. doi: 10.24963/IJCAI.2019/840.

Carta, T., Romac, C., Wolf, T., Lamprier, S., Sigaud, O., and Oudeyer, P.-Y. Grounding Large Language Models in Interactive Environments with Online Reinforcement Learning. In *Proceedings of the 40th International Conference on Machine Learning*, pp. 3676–3713. PMLR, July 2023.

Cho, K., van Merriënboer, B., Bahdanau, D., and Bengio, Y. On the Properties of Neural Machine Translation: Encoder–Decoder Approaches. In *Proceedings of SSST-8, Eighth Workshop on Syntax, Semantics and Structure in Statistical Translation*, pp. 103–111. Association for Computational Linguistics, 2014. doi: 10.3115/v1/W14-4012.

Cloete, J., Jackermeier, M., Havoutis, I., and Abate, A. PlatoLTL: Learning to generalize across symbols in LTL instructions for multi-task RL. *arXiv*, January 2026.

Crouse, M., Abdelaziz, I., Cornelio, C., Thost, V., Wu, L., Forbus, K., and Fokoue, A. Improving Graph Neural Network Representations of Logical Formulae with Subgraph Pooling, 2020.

Evans, R., Saxton, D., Amos, D., Kohli, P., and Grefenstette, E. Can Neural Networks Understand Logical Entailment? In *International Conference on Learning Representations*, 2018.

Goyal, P., Niekum, S., and Mooney, R. J. Using natural language for reward shaping in reinforcement learning. In *Proceedings of the 28th International Joint Conference on Artificial Intelligence, IJCAI’19*, pp. 2385–2391. AAAI Press, 2019. ISBN 978-0-9992411-4-1.

Guo, Z., Işık, İ., Ahmad, H. M. S., and Li, W. One Subgoal at a Time: Zero-Shot Generalization to Arbitrary Linear Temporal Logic Requirements in Multi-Task Reinforcement Learning. In *The Thirty-ninth Annual Conference on Neural Information Processing Systems*, October 2025.

Hahn, E. M., Perez, M., Schewe, S., Somenzi, F., Trivedi, A., and Wojtczak, D. Omega-Regular Objectives in Model-Free Reinforcement Learning. In *Tools and Algorithms for the Construction and Analysis of Systems*, pp. 395–412, 2019. ISBN 978-3-030-17462-0. doi: 10.1007/978-3-030-17462-0_27.

Hasanbeig, M., Abate, A., and Kroening, D. Logically-Constrained Reinforcement Learning. *arXiv*, 2018. doi: 10.48550/arXiv.1801.08099.

Hill, F., Mokra, S., Wong, N., and Harley, T. Human Instruction-Following with Deep Reinforcement Learning via Transfer-Learning from Text. In *arXiv*, May 2020. doi: 10.48550/arXiv.2005.09382.

Jackermeier, M. and Abate, A. DeepLTL: Learning to efficiently satisfy complex LTL specifications for multi-task RL. In *International Conference on Learning Representations (ICLR)*, 2025.

Jothismurgan, K., Bansal, S., Bastani, O., and Alur, R. Compositional Reinforcement Learning from Logical Specifications. In *Advances in Neural Information Processing Systems*, volume 34, pp. 10026–10039, 2021.

Kingma, D. P. and Ba, J. Adam: A method for stochastic optimization. In Bengio, Y. and LeCun, Y. (eds.), *3rd International Conference on Learning Representations*, 2015. doi: 10.48550/arXiv.1412.6980.

Klissarov, M., Henaff, M., Raileanu, R., Sodhani, S., Vincent, P., Zhang, A., Bacon, P.-L., Precup, D., Machado, M. C., and D’Oro, P. MaestroMotif: Skill Design from Artificial Intelligence Feedback. In *The Thirteenth International Conference on Learning Representations*, 2025.

Kuo, Y.-L., Katz, B., and Barbu, A. Encoding formulas as deep networks: Reinforcement learning for zero-shot execution of LTL formulas. In *2020 IEEE/RSJ International Conference on Intelligent Robots and Systems (IROS)*, pp. 5604–5610, October 2020. doi: 10.1109/IROS45743.2020.9341325.

Le, X.-B., Wagner, D., Witzman, L., Rabinovich, A., and Ong, L. Reinforcement Learning with LTL and ω -Regular Objectives via Optimality-Preserving Translation to Average Rewards. In *The Thirty-eighth Annual Conference on Neural Information Processing Systems*, November 2024.

León, B. G., Shanahan, M., and Belardinelli, F. Systematic Generalisation through Task Temporal Logic and Deep Reinforcement Learning. In *arXiv*. arXiv, 2021. doi: 10.48550/arXiv.2006.08767.

León, B. G., Shanahan, M., and Belardinelli, F. In a Nutshell, the Human Asked for This: Latent Goals for Following Temporal Specifications. In *International Conference on Learning Representations*, 2022.

Liu, J. X., Shah, A., Rosen, E., Jia, M., Konidaris, G., and Tellex, S. Skill Transfer for Temporal Task Specification. In *2024 IEEE International Conference on Robotics and Automation (ICRA)*, pp. 2535–2541, 2024. doi: 10.1109/ICRA57147.2024.10611432.

Liu, M., Zhu, M., and Zhang, W. Goal-Conditioned Reinforcement Learning: Problems and Solutions. In *Proceedings of the Thirty-First International Joint Conference on Artificial Intelligence*, pp. 5502–5511, July 2022. ISBN 978-1-956792-00-3. doi: 10.24963/ijcai.2022/770.

Luketina, J., Nardelli, N., Farquhar, G., Foerster, J. N., Andreas, J., Grefenstette, E., Whiteson, S., and Rocktäschel, T. A survey of reinforcement learning informed by natural language. In *Proceedings of the Twenty-Eighth International Joint Conference on Artificial Intelligence*, pp. 6309–6317, 2019. doi: 10.24963/IJCAI.2019/880.

McCluskey, E. J. Minimization of boolean functions. *The Bell System Technical Journal*, 35(6):1417–1444, 1956.

Oh, J., Singh, S., Lee, H., and Kohli, P. Zero-Shot Task Generalization with Multi-Task Deep Reinforcement Learning. In *Proceedings of the 34th International Conference on Machine Learning*, pp. 2661–2670. PMLR, July 2017.

Pagliari, D., Cupiał, B., Coward, S., Piterbarg, U., Włoczyk, M., Khan, A., Pignatelli, E., Kuciński, Ł., Pinto, L., Fergus, R., Foerster, J. N., Parker-Holder, J., and Rocktäschel, T. BALROG: Benchmarking Agentic LLM and VLM Reasoning On Games. In *The Thirteenth International Conference on Learning Representations*, 2025.

Pnueli, A. The temporal logic of programs. In *18th Annual Symposium on Foundations of Computer Science (SFCS 1977)*, pp. 46–57, October 1977. doi: 10.1109/SFCS.1977.32.

Press, O., Smith, N., and Lewis, M. Train Short, Test Long: Attention with Linear Biases Enables Input Length Extrapolation. In *International Conference on Learning Representations*, October 2021.

Qiu, W., Mao, W., and Zhu, H. Instructing Goal-Conditioned Reinforcement Learning Agents with Temporal Logic Objectives. In *Thirty-Seventh Conference on Neural Information Processing Systems*, November 2023.

Quine, W. V. The problem of simplifying truth functions. *The American Mathematical Monthly*, 59(8):521–531, 1952.

Sadigh, D., Kim, E. S., Coogan, S., Sastry, S. S., and Seshia, S. A. A learning based approach to control synthesis of Markov decision processes for linear temporal logic specifications. In *53rd IEEE Conference on Decision and Control*, pp. 1091–1096, December 2014. doi: 10.1109/CDC.2014.7039527.

Schlichtkrull, M. S., Kipf, T. N., Bloem, P., van den Berg, R., Titov, I., and Welling, M. Modeling relational data with graph convolutional networks. In *ESWC*, volume 10843 of *Lecture Notes in Computer Science*, pp. 593–607. Springer, 2018.

Schulman, J., Wolski, F., Dhariwal, P., Radford, A., and Klimov, O. Proximal Policy Optimization Algorithms. *arXiv*, (preprint), August 2017. doi: 10.48550/arXiv.1707.06347.

Shah, A., Voloshin, C., Yang, C., Verma, A., Chaudhuri, S., and Seshia, S. A. LTL-Constrained Policy Optimization with Cycle Experience Replay. *Transactions on Machine Learning Research*, 2025.

Shao, D. and Kwiatkowska, M. Sample efficient model-free reinforcement learning from LTL specifications with optimality guarantees. In *Proceedings of the Thirty-Second International Joint Conference on Artificial Intelligence*, pp. 4180–4189, 2023. doi: 10.24963/IJCAI.2023/465.

Sickert, S., Esparza, J., Jaax, S., and Křetínský, J. Limit-Deterministic Büchi Automata for Linear Temporal Logic. In *Computer Aided Verification*, Lecture Notes in Computer Science, pp. 312–332, 2016. ISBN 978-3-319-41540-6. doi: 10.1007/978-3-319-41540-6_17.

Vaezipoor, P., Li, A. C., Icarte, R. A. T., and Mcilraith, S. A. LTL2Action: Generalizing LTL Instructions for Multi-Task RL. In *Proceedings of the 38th International Conference on Machine Learning*, pp. 10497–10508. PMLR, July 2021.

Vaswani, A., Shazeer, N., Parmar, N., Uszkoreit, J., Jones, L., Gomez, A. N., Kaiser, L., and Polosukhin, I. Attention is all you need. In *Annual Conference on Neural Information Processing Systems 2017*, pp. 5998–6008, 2017.

Voloshin, C., Verma, A., and Yue, Y. Eventual Discounting Temporal Logic Counterfactual Experience Replay. In *Proceedings of the 40th International Conference on Machine Learning*, pp. 35137–35150. PMLR, July 2023.

Zaheer, M., Kottur, S., Ravanbakhsh, S., Poczos, B., Salakhutdinov, R. R., and Smola, A. J. Deep Sets. In *Advances in Neural Information Processing Systems*, volume 30, 2017.



Figure 4. Visualisation of environments. (a) In ZoneEnv the agent has to navigate between zones of different colours. (b) In the Warehouse environment, the agent has to move crates and vases to different regions. In both environments, the agent receives lidar observations and outputs continuous actions for acceleration and steering.

A. Semantics of LTL

The satisfaction semantics of LTL are specified by the satisfaction relation $\sigma \models \varphi$, which is recursively defined as follows (Pnueli, 1977):

$$\begin{aligned}
 \sigma \models \top & \\
 \sigma \models a & \text{ iff } a \in \sigma_0 \\
 \sigma \models \varphi \wedge \psi & \text{ iff } \sigma \models \varphi \wedge \sigma \models \psi \\
 \sigma \models \neg \varphi & \text{ iff } \sigma \not\models \varphi \\
 \sigma \models X \varphi & \text{ iff } \sigma_1 \dots \models \varphi \\
 \sigma \models \varphi \cup \psi & \text{ iff } \exists j \geq 0. \sigma_j \dots \models \psi \wedge \forall 0 \leq i < j. \sigma_i \dots \models \varphi.
 \end{aligned}$$

B. Algorithm to Identify Accepting Runs

Algorithm 1 presents the DFS-based procedure from Jäckermeier & Abate (2025) for computing paths from a given LDBA state to accepting cycles. This yields a set of accepting runs that we then convert to sequences of Boolean formulae. We employ two practical optimisations during this conversion process: first, as observed by Jäckermeier & Abate (2025), requiring the policy to avoid *all* other LDBA states $q \notin \{q_i, q_{i+1}\}$ at step i can be overly restrictive. Instead, we construct β_i^- to only avoid assignments that lead to: (i) sink states (states from which satisfying the specification is impossible), or (ii) previous states on the current path (which would undo progress). This relaxation allows the policy more flexibility while still preventing catastrophic transitions. Second, when a positive formula β_i^+ contains a disjunction, we generate a separate formula sequence for each disjunct in β_i^+ . This avoids requiring the policy to internally select between the different options. Instead, we employ the value function to choose the approximately optimal formula sequences as described in Section 4.4.

C. Experimental Details

C.1. Environments

ZoneEnv. The ZoneEnv environment was introduced by Vaezipoor et al. (2021). It consists of a walled plane with 8 circular regions (“zones”) that have four different colours and form the atomic propositions. Since the zones never overlap, the assignments all correspond to singleton sets of atomic propositions (or the empty set). It features a 2-dimensional continuous action space for acceleration and steering. The environment features a high-dimensional state space based on lidar information about the zones, and data from other sensors. Both the zone and robot positions are randomly sampled at the beginning of each episode. If the agent at any point touches a wall, the episode is terminated prematurely. A visualisation of the ZoneEnv environment is provided in Figure 4a.

Warehouse. The warehouse environment consists of a continuous state space, on which a point agent moves via continuous actions. The agent can interact with two types of objects: crates and vases. Both the agent position and the object positions are randomly sampled at the beginning of each episode. There are furthermore three different fixed regions in the grid: region A (red), region B (green), and door (purple). The agent observes objects via a lidar sensor, and additionally receives directional information about the regions. The action space is composite: at each step, the agent can apply both a continuous

Algorithm 1 Computing paths to accepting cycles (Jackermeier & Abate, 2025)

Require: LDBA $B = (\mathcal{Q}, q_0, \Sigma, \delta, \mathcal{E}, \mathcal{F})$ and current state q .

- 1: **function** $\text{DFS}(q, p, i)$ $\{i$ is index of last seen accepting state, or $-1\}$
- 2: $P \leftarrow \emptyset$
- 3: **if** $q \in \mathcal{F}$ **then**
- 4: $i \leftarrow |p|$
- 5: **end if**
- 6: **for all** $a \in \Sigma \cup \{\varepsilon\}$ **do**
- 7: $p' \leftarrow [p, q]$
- 8: $q' \leftarrow \delta(q, a)$
- 9: **if** $q' \in p$ **then**
- 10: **if** index of q' in $p \leq i$ **then**
- 11: $P \leftarrow P \cup \{p'\}$
- 12: **end if**
- 13: **else**
- 14: $P \leftarrow P \cup \text{DFS}(q', p', i)$
- 15: **end if**
- 16: **end for**
- 17: **return** P
- 18: **end function**
- 19: $\{\text{Main entry point}\}$
- 20: **if** $q \in \mathcal{F}$ **then**
- 21: $i \leftarrow 0$
- 22: **else**
- 23: $i \leftarrow -1$
- 24: **end if**
- 25: **return** $\text{DFS}(q, [], i)$

Table 2. Possible assignments in the Warehouse environment.

$\{\text{region_a}\}$	$\{\text{region_b}\}$	$\{\text{door}\}$
$\{\text{vase}\}$	$\{\text{crate}\}$	$\{\text{region_a, vase}\}$
$\{\text{region_a, crate}\}$	$\{\text{region_b, vase}\}$	$\{\text{region_b, crate}\}$
$\{\text{door, vase}\}$	$\{\text{door, crate}\}$	$\{\text{vase, crate}\}$
$\{\text{region_a, vase, crate}\}$	$\{\text{region_b, vase, crate}\}$	$\{\text{door, vase, crate}\}$
		\emptyset

movement action and pick up or drop a crate or vase. The atomic propositions specify whether the agent is currently carrying a vase or a crate, and if the agent is in one of the three regions. Table 2 lists all possible combinations of propositions that hold true at some state in the Warehouse environment. See Figure 4b for a visualisation of the environment.

C.2. Training Curricula

We develop a generic training curriculum for each environment, detailed in Table 3. Each curriculum stage consists of a distribution over sequences of Boolean formulae in DNF. Later curriculum stages generally consist of more difficult tasks. Once the agent has achieved sufficient success on tasks sampled from the current stage (as measured by successes over the last 256 episodes), we move on to the next stage. We define four general, environment-independent sets of formulae used to construct the curricula: PROPS are simply formulae of the form p , where $p \in AP$. AND consists of conjunctions of propositions up to length 3. ANDNOT consists of formulae of the form $p_1 \wedge \neg p_2$. Finally, OR consists of disjunctions of all possible formulae from the previous sets. We furthermore distinguish two sequence types: REACH-AVOID sequences of the form $((\beta_1^+, \beta_1^-), \dots, (\beta_n^+, \beta_n^-))$ and REACH-STAY sequences $((\beta_\varepsilon, \beta_1^-), (\varphi, \neg\varphi), (\varphi, \neg\varphi), \dots)$ that contain the ε -token β_ε and require the agent to at some point hold formula φ for n time steps. For DeepLTL we compute satisfying assignments for each formula in order to obtain a sequence of assignments, rather than a sequence of formulae.

Table 3. Curricula for training sequences. For each stage, we list the success rate threshold κ for progression (measured over a rolling window of the 256 latest episodes), the sequence type (reach-avoid/reach-stay), the probability P_{seq} of sampling a sequence of that type, the number of steps n in the sequence (or, for reach-stay tasks, the number of consecutive time steps for satisfying the “stay” sub-task), the type of each reach (β_i^+) and avoid (β_i^-) Boolean formula, and the probability P_{avoid} of sampling avoid formulae at each timestep. Dashes (—) indicate “not applicable”.

	STAGE	κ	TYPE	P_{seq}	n	β_i^+	β_i^-	P_{avoid}
ZONEENV	1	0.9	REACH-AVOID	1.0	1	PROPS	—	0.0
	2	0.95	REACH-AVOID	1.0	2	PROPS	—	0.0
	3	0.95	REACH-AVOID	1.0	1	PROPS	PROPS	1.0
	4	0.9	REACH-AVOID	1.0	2	PROPS	PROPS	1.0
	5	0.9	REACH-AVOID	0.4	[1, 2]	PROPS	PROPS+ORs	0.7
			REACH-STAY	0.6	30	PROPS	PROPS	0.5
	6	0.9	REACH-AVOID	0.8	[1, 2]	PROPS	PROPS+ORs	0.7
			REACH-STAY	0.2	60	PROPS	PROPS	0.5
WAREHOUSE	1	0.9	REACH-AVOID	1.0	1	PROPS	—	0.0
	2	0.95	REACH-AVOID	1.0	1	ALL EXCEPT ORs	—	0.0
	3	0.9	REACH-AVOID	1.0	2	ALL EXCEPT ORs	—	0.0
	4	0.95	REACH-AVOID	1.0	1	ALL EXCEPT ORs	ALL EXCEPT ORs	0.5
	5	0.95	REACH-AVOID	1.0	[1,2]	ALL EXCEPT ORs	ALL EXCEPT ORs	0.5
	6	0.9	REACH-AVOID	0.4	[1, 2]	ALL EXCEPT ORs	ALL	0.5
			REACH-STAY	0.6	30	ALL EXCEPTS ORs	ALL EXCEPT ORs	0.2
	7	—	REACH-AVOID	0.8	[1, 2]	ALL EXCEPT ORs	ALL	0.5
			REACH-STAY	0.2	60	ALL EXCEPT ORs	ALL	0.5

LTL2Action does not originally employ curriculum learning, but we experimented with various training curricula for a fair comparison. We found it important to include diverse LTL formulae even in early curriculum stages (in contrast to the curricula for the other methods), since LTL2Action operates directly on the syntax level and hence requires exposure to all the various LTL operators. In ZoneEnv, we sample formulae of the reach-avoid family of the form $\neg a \cup ((b \vee c) \wedge \dots)$ with increasing depth and number of disjunctions in later curriculum stages. We use the same family for the Warehouse curriculum, but furthermore sample Boolean formulae from the AND and ANDNOT families instead of simple atomic propositions in later stages. Note that LTL2Action does not support infinite-horizon specifications, and we hence do not sample formulae containing the G operator.

C.3. Hyperparameters

Table 4 lists hyperparameters of StructLTL and the baselines. We report PPO parameters and details on the neural network architectures used for processing environment observations and the actor and critic. ZoneEnv hyperparameters were chosen to match previous work (Vaezipoor et al., 2021; Jackermeier & Abate, 2025) and adapted for the Warehouse environment. We use the Adam optimiser (Kingma & Ba, 2015) throughout.

Model architectures. All methods employ the same overall model architecture. Environment observations are encoded with an MLP and the current LTL task is encoded in a method-dependent way (see below). The resulting latent representations are then concatenated and fed through actor and critic MLPs, respectively. The critic directly outputs a scalar estimate of the value function, whereas the actor outputs the parameters of the action distribution. In ZoneEnv, the actor consists of an MLP with two output heads for the mean and standard deviation of a diagonal Gaussian. In Warehouse, the actor MLP additionally produces logits for a categorical distribution over the discrete actions. Finally, for StructLTL and DeepLTL the actor MLP additionally has a head that outputs the log-probability of taking an ε -action.

Table 4. Hyperparameters for LTL2Action, DeepLTL, and StructLTL across ZoneEnv and Warehouse. Values spanning multiple columns indicate identical settings across those methods/environments.

Category	Hyperparameter	ZoneEnv			WarehouseEnv		
		LTL2Action	DeepLTL	StructLTL	LTL2Action	DeepLTL	StructLTL
PPO	Total timesteps	—	5×10^6	—	—	2×10^8	—
	Environments	—	16	—	64	—	128
	Steps/update	—	4096	—	—	1024	—
	Minibatches	—	32	—	—	4	—
	Update epochs	—	10	—	—	5	—
	Discount (γ)	—	0.998	—	—	—	—
	GAE lambda (λ)	—	0.95	—	—	—	—
	Clip epsilon	—	0.2	—	—	—	—
	Entropy coef.	—	0.003	—	—	—	—
	Value func. coef.	—	0.5	—	—	—	—
Curriculum	Learning rate	—	3×10^{-4}	—	—	5×10^{-4}	—
	Max grad norm	—	0.5	—	—	1.0	—
	Adam epsilon	—	—	10^{-8}	—	—	—
Env Net	Episode window	—	256	—	—	—	—
Actor	Hidden sizes	—	—	[128]	—	—	—
	Output size	—	—	64	—	—	—
	Activation	—	—	Tanh	—	—	—
Critic	Hidden sizes	—	—	[64, 64]	—	—	—
	Activation	—	—	Tanh	—	—	—
Environment	Max episode length	—	—	1,000	—	—	—

LTL encoding networks. LTL2Action encodes the LTL formula using a relational graph convolutional network (RGCN; Schlichtkrull et al., 2018) applied to the formula’s syntax tree. Following the original paper, it consists of 8 layers with Tanh activations, using an embedding dimension of 32 for ZoneEnv and 16 for Warehouse. The weights of all layers are shared, and each layer receives as input the output from the previous layer concatenated with the original one-hot encodings of the symbols in the syntax tree.

DeepLTL encodes sequences of sets of assignments using 16-dimensional embeddings (one for each assignment) processed by a DeepSets module (Zaheer et al., 2017) with a hidden layer size of 32 and an output size of 16, using ReLU activations and summation as the aggregation mechanism. The encoded reach and avoid sets are then concatenated and processed with a gated recurrent unit (GRU; Cho et al., 2014) with embedding size 32. The GRU is applied back-to-front, and the final hidden state forms the sequence embedding. We use $k = 2$ (the number of repeating loops at test time) throughout.

StructLTL uses 16-dimensional proposition embeddings and processes clauses and disjuncts with separate DeepSets networks, both with no hidden layers, output size 16, and ReLU activations. The attention mechanism uses hidden dimension $d_k = 32$ and ALiBi slope $m = 0.5$ in ZoneEnv, and $m = 5.0$ in Warehouse. As in DeepLTL, we set $k = 2$.

C.4. Evaluation Tasks

Table 5 lists the complete LTL specifications used in our evaluation. The ZoneEnv tasks are based on established specifications from the literature (Jackermeier & Abate, 2025). Warehouse tasks were designed to encompass a broad range of interesting behaviour (such as transporting objects to different regions) and LTL structures.

D. Ablation Studies

D.1. Impact of Hierarchical DNF Encoder

In this ablation study, we investigate the impact of our proposed hierarchical DNF encoder. In particular, we replace the DNF encoder with a flat sequence model that processes Boolean formulae as lists of tokens. We choose a gated recurrent

Table 5. Complete list of evaluation specifications.

ID	Environment	LTL Formula
<i>Finite Horizon</i>		
φ_1	ZoneEnv	$F(\text{green} \wedge (\neg\text{red} \mathbin{U} \text{yellow})) \wedge F \text{purple}$
φ_2	ZoneEnv	$(F \text{red}) \wedge (\neg\text{red} \mathbin{U} (\text{green} \wedge F \text{yellow}))$
φ_3	ZoneEnv	$F(\text{red} \vee \text{green}) \wedge F \text{yellow} \wedge F \text{purple}$
φ_4	ZoneEnv	$\neg(\text{purple} \vee \text{yellow}) \mathbin{U} (\text{red} \wedge F \text{green})$
φ_5	ZoneEnv	$\neg\text{green} \mathbin{U} ((\text{red} \vee \text{purple}) \wedge (\neg\text{green} \mathbin{U} \text{yellow}))$
φ_6	ZoneEnv	$((\text{green} \vee \text{red}) \rightarrow (\neg\text{yellow} \mathbin{U} \text{purple})) \mathbin{U} \text{yellow}$
φ_7	Warehouse	$F(\text{region_a} \wedge F(\text{crate} \wedge F \text{region_b}))$
φ_8	Warehouse	$\neg(\text{region_a} \vee \text{door}) \mathbin{U} (\text{vase} \wedge \text{region_b})$
φ_9	Warehouse	$\neg\text{door} \mathbin{U} (\text{region_a} \wedge (\neg\text{vase} \mathbin{U} \text{region_b}))$
φ_{10}	Warehouse	$\neg(\text{vase} \vee \text{crate}) \mathbin{U} (\text{region_a} \wedge F(\text{door} \wedge F \text{region_b}))$
φ_{11}	Warehouse	$F(\text{vase} \wedge \text{region_a} \wedge (\text{region_a} \mathbin{U} (\neg\text{vase} \wedge \text{region_a})))$
φ_{12}	Warehouse	$F(\text{vase} \wedge \text{crate} \wedge \text{region_b} \wedge (\text{region_b} \mathbin{U} (\neg\text{vase} \wedge \neg\text{crate} \wedge \text{region_b})))$
φ_{13}	Warehouse	$(\text{crate} \rightarrow (\text{crate} \mathbin{U} \text{region_b})) \mathbin{U} (\text{crate} \wedge \text{region_b} \wedge (\text{region_b} \mathbin{U} (\neg\text{crate} \wedge \text{region_b})))$
φ_{14}	Warehouse	$(\text{vase} \rightarrow (\text{vase} \mathbin{U} \text{door})) \mathbin{U} (F(\text{crate} \wedge \text{region_b} \wedge (\text{region_b} \mathbin{U} (\neg\text{crate} \wedge \text{region_b}))) \wedge F(\text{vase} \wedge \text{door} \wedge (\text{door} \mathbin{U} (\neg\text{vase} \wedge \text{door}))))$
φ_{15}	Warehouse	$(\text{crate} \rightarrow (\neg(\text{region_a} \vee \text{region_b}) \mathbin{U} \text{door})) \mathbin{U} (\text{vase} \wedge \text{door} \wedge (\text{door} \mathbin{U} (\neg\text{vase} \wedge \text{door})))$
φ_{16}	Warehouse	$F(\text{crate} \wedge \text{region_a} \wedge (\text{region_a} \mathbin{U} (\neg\text{crate} \wedge \text{region_a}))) \wedge F(\text{vase} \wedge \text{door} \wedge (\text{door} \mathbin{U} (\neg\text{vase} \wedge \text{door})))$
<i>Infinite Horizon</i>		
ψ_1	ZoneEnv	$G F \text{yellow} \wedge G F \text{green}$
ψ_2	ZoneEnv	$G F \text{red} \wedge G F \text{green} \wedge G F \text{yellow} \wedge G \neg\text{purple}$
ψ_3	ZoneEnv	$F G \text{red}$
ψ_4	ZoneEnv	$F G \text{red} \wedge F(\text{yellow} \wedge F \text{green})$
ψ_5	ZoneEnv	$F G \text{purple} \wedge G \neg\text{yellow}$
ψ_6	ZoneEnv	$G((\text{green} \vee \text{yellow}) \rightarrow F \text{red}) \wedge F G(\text{green} \vee \text{purple})$
ψ_7	Warehouse	$G F(\text{region_a} \wedge G F \text{region_b} \wedge G F \text{door})$
ψ_8	Warehouse	$G F(\text{vase} \wedge F \neg\text{vase}) \wedge G F(\text{crate} \wedge F \neg\text{crate}) \wedge G \neg\text{region_a}$
ψ_9	Warehouse	$F(\text{vase} \wedge \text{region_a} \wedge (\text{region_a} \mathbin{U} (\neg\text{vase} \wedge \text{region_a}))) \wedge G F \text{door} \wedge G F \text{region_b}$
ψ_{10}	Warehouse	$G F(\text{vase} \wedge \text{region_a} \wedge (\text{region_a} \mathbin{U} (\neg\text{vase} \wedge \text{region_a}))) \wedge G F(\text{crate} \wedge \text{region_b} \wedge (\text{region_b} \mathbin{U} (\neg\text{crate} \wedge \text{region_b})))$
ψ_{11}	Warehouse	$F G \text{region_a}$
ψ_{12}	Warehouse	$F(\text{vase} \wedge \text{region_b} \wedge (\text{region_b} \mathbin{U} (\neg\text{vase} \wedge \text{region_b}))) \wedge F G \text{region_b}$
ψ_{13}	Warehouse	$F G(\text{crate} \wedge \text{region_a})$
ψ_{14}	Warehouse	$F G(\text{vase} \wedge \text{region_b}) \wedge G \neg\text{region_a} \wedge G \neg\text{crate}$
ψ_{15}	Warehouse	$G((\text{door} \vee \text{region_b}) \rightarrow F \text{region_a}) \wedge F G(\text{vase} \vee \text{crate})$
ψ_{16}	Warehouse	$F G \text{crate} \wedge G(\text{vase} \rightarrow F(\text{door} \wedge \neg\text{crate}))$

unit (GRU; Cho et al., 2014) for this study and only consider the Warehouse environment, since ZoneEnv does not admit complex Boolean formula sequences. For a fair comparison, we set the embedding size of the tokens to 16, as in our main experiments. Note that we only replace the encoding of Boolean formulae themselves, in order to precisely ablate this part of our proposed architecture; the higher-level sequence encoding is still accomplished with our proposed attention mechanism.

The results in Figure 5a clearly demonstrate that our hierarchical DNF encoding scheme is superior to flat token-based encodings of the Boolean formula. While token-based encodings show some success, the policy fails to learn useful representations as it progresses through the curriculum and encounters more complex Boolean formulae. In contrast, our hierarchical encoding mechanism achieves high success rates.

D.2. Impact of Temporal Attention Mechanism

We proceed to investigate the impact of the temporal attention mechanism. We compare our proposed approach to (i) a myopic baseline that only conditions on the first step of the Boolean formula sequence, and (ii) encoding the sequence of Boolean formulae with a GRU instead of attention. We conduct this ablation study in the ZoneEnv environment.

Figure 5b shows that our proposed attention mechanism performs better than the alternatives. The myopic baseline initially learns quickly, but then plateaus. The GRU converges slightly above the myopic baseline, but below the attention method.

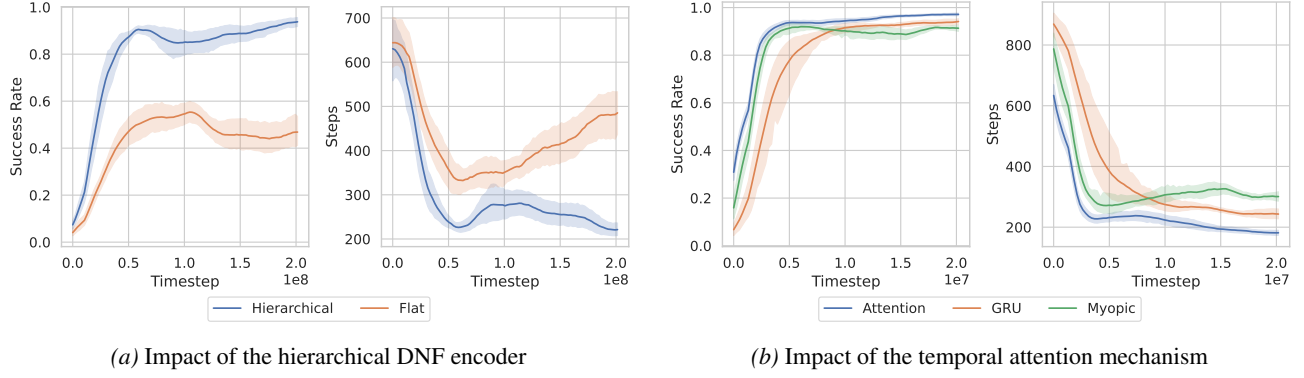


Figure 5. Ablation studies. We report averages over finite-horizon evaluation tasks, computed over 50 episodes per task. Shaded areas indicate 90% confidence intervals over 10 random seeds.

D.3. Variation of Success Rate with Increasing Number of Possible Assignments

In this ablation study, we investigate the robustness of our approach to increasing numbers of possible assignments. We consider variations of the Warehouse environment that use subsets of the possible propositions from $\{\text{region_a, region_b, door, vase, crate}\}$, and thus subsets of the assignments in Table 2. The simplest variation considers only one region and one object, i.e. $\{\text{region_a, vase}\}$, and the other variations increase the number of regions and/or objects up to the full Warehouse environment with 3 regions and 2 objects. To investigate specifically the effect of the number of assignments and not the general environment complexity, the MDP \mathcal{M} is kept the same for all variations (e.g. a variation without crate will still contain crate objects that the agent can see and pick/place, but the labelling function $L(s)$ will not consider them). We train StructLTL and DeepLTL on each variation of Warehouse, and evaluate them on applicable (i.e. only containing valid propositions) finite-horizon LTL specifications from Table 6 during training. We omit LTL2Action from this ablation study, due to its generally poor performance.

Figure 6 presents the results. We see that for both methods, increasing the number of possible assignments decreases the rate of convergence. However, this decrease in rate of convergence is greater for DeepLTL compared to StructLTL. Moreover, the success rate of DeepLTL at convergence generally decreases as the number of possible assignments increases, while StructLTL is robust to this change and maintains very high success rates for all variations.

This confirms that the structured representations learned by StructLTL are able to better generalise across complex specifications compared to existing methods such as DeepLTL, which struggle with the combinatorial explosion of assignments.

E. Trajectory Visualisations

Figures 7 and 8 show trajectories produced by StructLTL on various specifications in ZoneEnv and Warehouse, respectively. The trajectories were obtained by executing the final policy at the end of training conditioned on the given tasks, and confirm that the policy correctly satisfies diverse specifications.

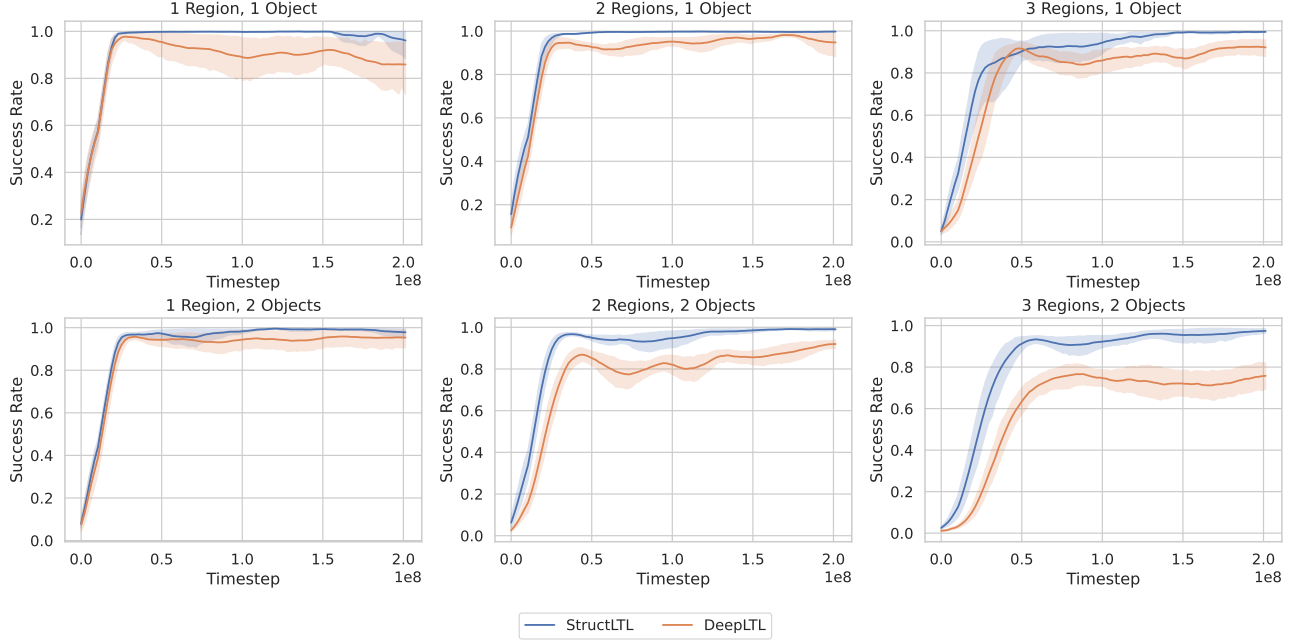
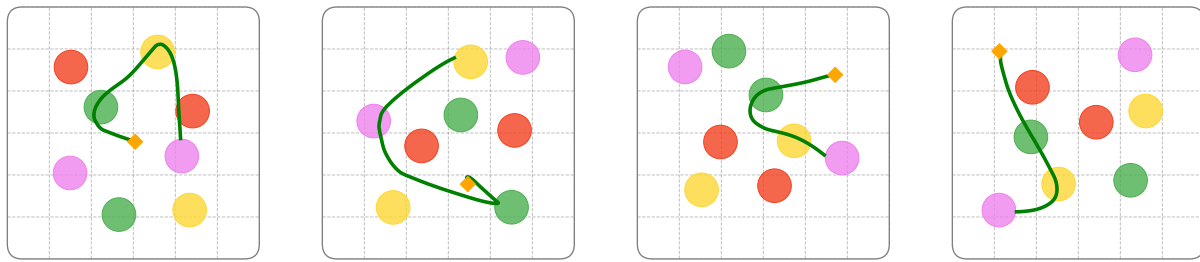


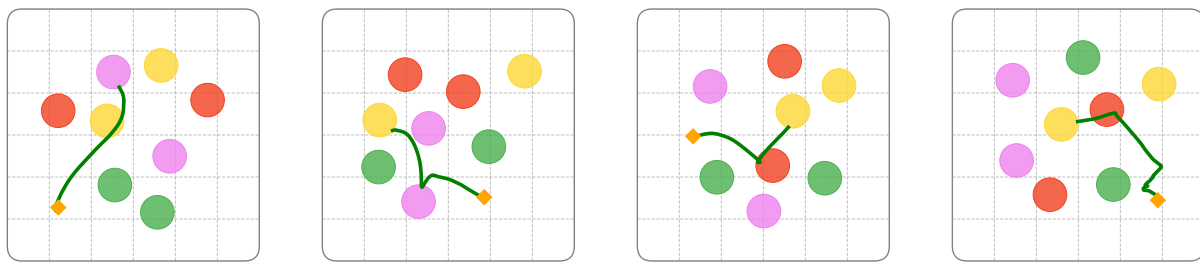
Figure 6. Success rates on finite-horizon tasks over training for different variations of the Warehouse environment. We report averages over the applicable finite-horizon evaluation tasks from Table 6, computed over 50 episodes per task. Shaded areas indicate 90% confidence intervals over 10 random seeds.

Table 6. Finite-horizon LTL specifications used for evaluation in the Warehouse environment for the ablation study in Appendix D.3. Note that since the different variations of the environment use subsets of the possible propositions (and thus subsets of the assignments in Table 2), each variation is only evaluated on the subset of valid specifications from this table.

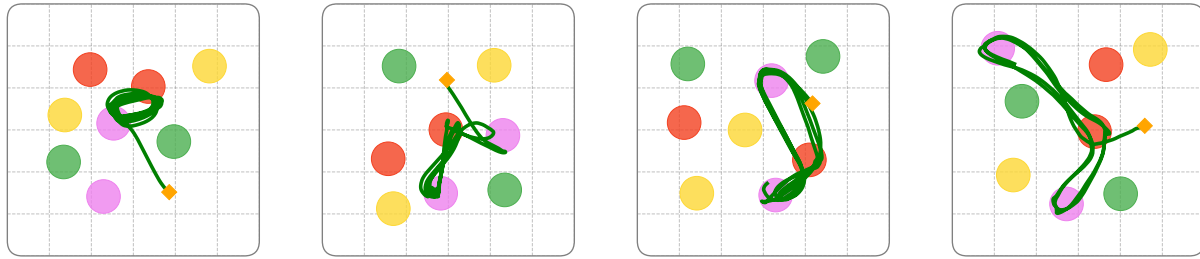
$F(vase \wedge \text{region_a} \wedge X(\neg(vase) \wedge \text{region_a}))$
$F(vase \wedge \text{region_b} \wedge X(\neg(vase) \wedge \text{region_b}))$
$F(vase \wedge \text{door} \wedge X(\neg(vase) \wedge \text{door}))$
$F(\text{crate} \wedge \text{region_a} \wedge X(\neg(\text{crate}) \wedge \text{region_a}))$
$F(\text{crate} \wedge \text{region_b} \wedge X(\neg(\text{crate}) \wedge \text{region_b}))$
$F(\text{crate} \wedge \text{door} \wedge X(\neg(\text{crate}) \wedge \text{door}))$
$F(vase \wedge \text{crate} \wedge \text{region_a} \wedge (\text{region_a} U (\neg(vase) \wedge \neg(\text{crate}) \wedge \text{region_a})))$
$F(vase \wedge \text{crate} \wedge \text{region_b} \wedge (\text{region_b} U (\neg(vase) \wedge \neg(\text{crate}) \wedge \text{region_b})))$
$F(vase \wedge \text{crate} \wedge \text{door} \wedge (\text{door} U (\neg(vase) \wedge \neg(\text{crate}) \wedge \text{door})))$
$F(vase \wedge \text{region_a} \wedge X(\neg(vase) \wedge \text{region_a})) \wedge G(vase \Rightarrow (vase U \text{region_a}))$



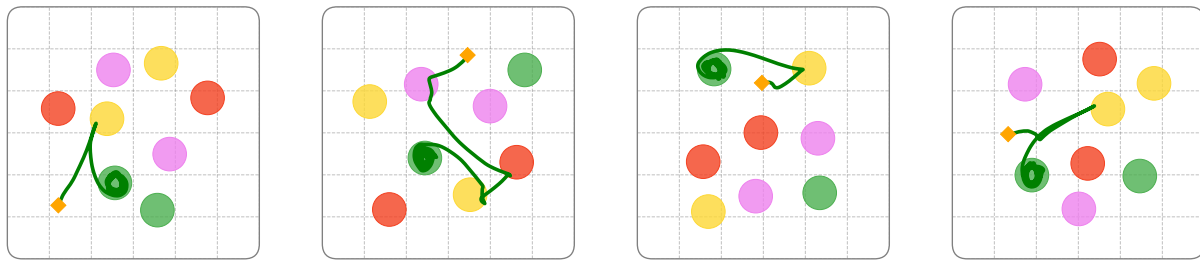
(a) $F(green \wedge \neg red \cup yellow) \wedge F purple$



(b) $F(red \vee purple) \wedge F yellow \wedge G \neg green$

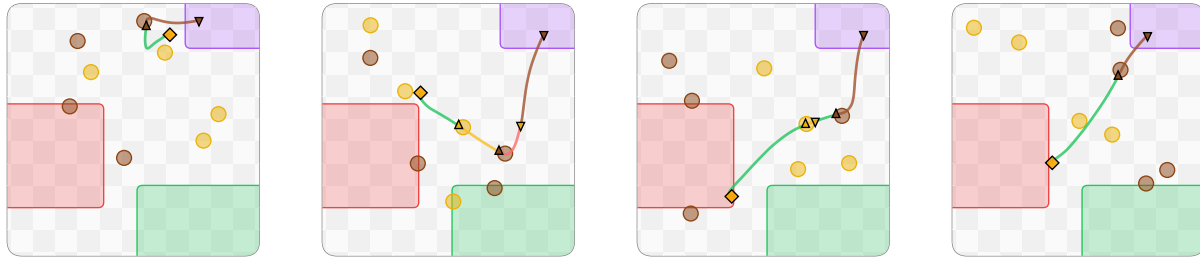


(c) $G F purple \wedge G F red \wedge G \neg yellow$

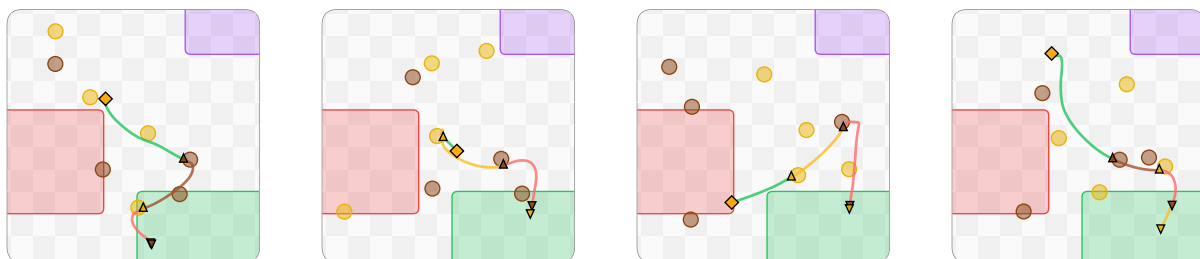


(d) $F yellow \wedge F G green \wedge G (purple \rightarrow F red)$

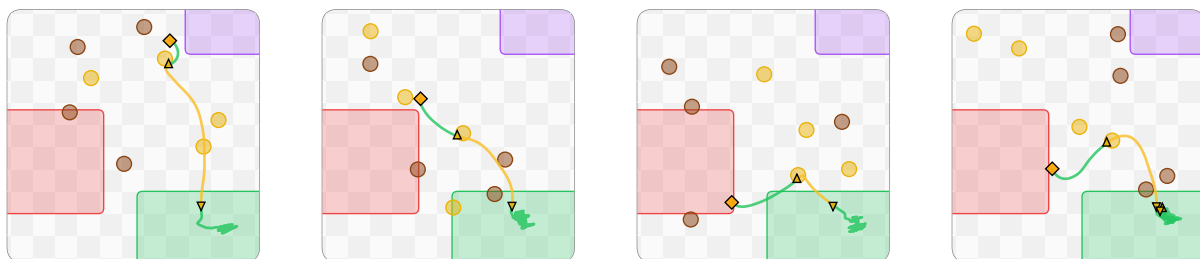
Figure 7. Example trajectories of StructLTL in ZoneEnv. The orange diamond indicates the starting position of the agent. All trajectories were generated by the same policy after training.



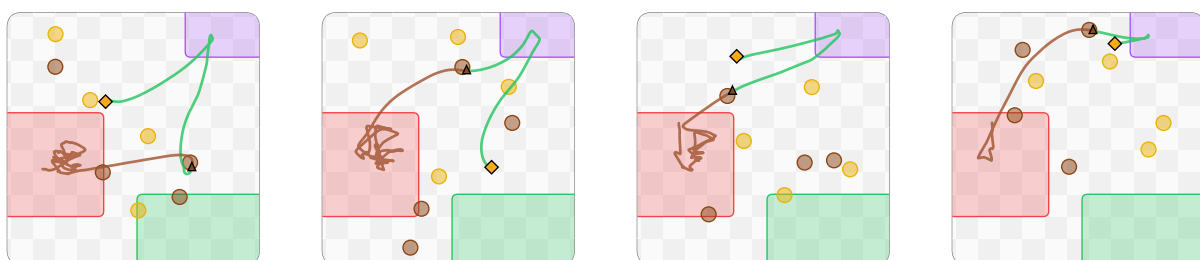
(a) $F (crate \wedge door \wedge (door \cup (\neg crate \wedge door)))$



(b) $F(vase \wedge crate \wedge region_b \wedge (region_b \cup (\neg vase \wedge \neg crate \wedge region_b)))$



(c) $F(vase \wedge \text{region_b} \wedge (\text{region_b} \cup (\neg \text{vase} \wedge \text{region_b}))) \wedge F G \text{region_b}$



(d) $F_{\text{door}} \wedge F_G(\text{crate} \wedge \text{region_a})$

Figure 8. Example trajectories of StructLTL in the Warehouse environment. The orange diamond indicates the starting position of the agent, and yellow and brown circles correspond to vases and crates, respectively. A triangle pointing upwards indicates picking up an object of the corresponding colour, while a triangle pointing downwards indicates dropping an object. Different trajectory colours similarly highlight the objects the agent is currently carrying. All trajectories were generated by the same policy after training.